Experimental and Numerical Study of a Building Retrofitting Solution Combining Phase Change Material Wallboards and Night Ventilation

Timea Béjat*[1] Emile Fulcheri[1], Didier Therme[1], Etienne Wurtz[1], Pierrick Péchambert[2]

1 Univ Grenoble Alpes, CEA, LITEN, DTS, LCEB, INES,
F-38000 Grenoble, France
**Corresponding author: timea.bejat@cea.fr*

2 Sainte Marie Constructions Isothermes (SMCI)
Zone Industrielle,
47220 Astaffort, France

ABSTRACT

The interest in phase change materials (PCMs) as a solution for thermal energy storage has been growing for the last decades. It is clear that PCMs are promising for reducing the summer heat peaks without increasing the energy demand for cooling. A new modular, reversible, lightweight retrofitting system was developed and integrated in a real size experimental test cell. The basic idea of the concept is to develop a retrofitting solution for office buildings which can be rapidly and reversibly installed as an inside layer on the existing structure, like a "box in a box" to replace air-conditioning by night cooling. It combines ventilated PCM panels with controlled shutters to manage incoming solar energy. Ventilation has two goals: decrease indoor air temperature, and solidify PCM. During the night, the PCM recovers its storage potential, which limits the increase in temperature the day after. The experimental analysis covers 8 months measurement campaign in real climate conditions. They show that the night ventilation of the PCM panels is efficient and allows a decrease in the inside temperature of about 3°C during summer nights. Average panel temperature is associated with a value of the thermal capacity of the PCM, thanks to the theoretical curve Cp(T) deduced from the technical data of the PCM. From the thermal capacities evaluated every minute, an average daily thermal capacity is calculated. Results of the paper show that the box in the box concept is able to replace air-condition by free cooling in temperate climates. Nevertheless, wise combination with space ventilation is crucial to obtain competitive results for hot periods. The simulations show that a PCM changing phase at 27 °C can decrease the "integrated thermal discomfort level over 26°C" (ITDL26) by 65% compared to a PCM changing phase at 23°C. Numerical analysis also emphasizes that rise the ventilation rate of the developed panels from 4 ACH to 8 ACH reduce the ITDL26 by 50%.

KEYWORDS

Phase change material (PCM), night ventilation, free cooling, building simulation, box in the box concept

1 INTRODUCTION

Organic PCMs such as paraffin or fatty acids seems the most interesting for building applications (low temperature) thanks to their high latent heat, their good chemical stability and their low supercooling (Zhang et al., 2006). PCM can be integrated in buildings in different ways, such as direct integration (mixed with the material of constructions), macro-encapsulation (important volumes directly integrated in panels, ducts or other container) and micro-encapsulation (integrated in very small capsules). When the PCM temperature is within its phase change range, it can store or release much more heat than a comparable mass of a typical sensible material. PCM can thus bring thermal mass to lightweight buildings while minimizing the additional thickness and thus the loss of space in the renovated room.

In this study, PCM panels are made of micro-encapsulated paraffin placed in an aluminium honeycomb matrix designed by CSTB (French Scientific and Technical Center for Buildings) (Hasse, 2011). The melting peak temperature of the used PCM is 23 °C. Figure 1 shows the

schema of the ventilated honeycomb wallboard. They contains PCM on room side and a ventilated cavity part on the backward.
The micro-encapsulation, the conductivity of aluminium and the specific structure of the matrix had been chosen to maximize the conductivity of the panel (Hasse, 2011). Hence the heat transfer between the PCM and both the air ventilated in the back of the PCM layer and the indoor air in the front is optimal.

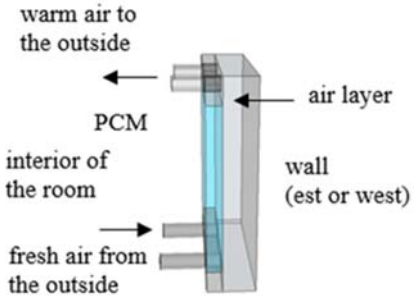

Figure 1: Illustration of the PCM panel

The first version of the studied system was developed by a previous consortium (Evola et al., 2011, Evola et al., 2014). As an improvement from that project, a ventilated air cavity was added to the wallboard to increase energy efficiency by ensuring daily regeneration of PCM.
In the studied system, a mechanical ventilation blows outdoor air into the panels to reach three goals:

- Cooling the panel and the indoor air during the night
- Solidifying the PCM to recover every night an important storage potential for the following day
- Improve summer thermal comfort of the room by keeping wall temperature on a constant or lower level than without the proposed technical solution.

The renovation system also includes VIP insulation panels (vacuum insulation technology) on opaque exterior walls, a double glazed window equipped with controlled blinds, in addition to the existing window. This latter assure the minimization of unwanted solar gains during the summer.

2 EXPERIMENTAL STUDY OF THE SYSTEM

The complete system was built at CEA INES's INCAS experimental platform. The schema of principle and the built systems are presented in Figure 2.

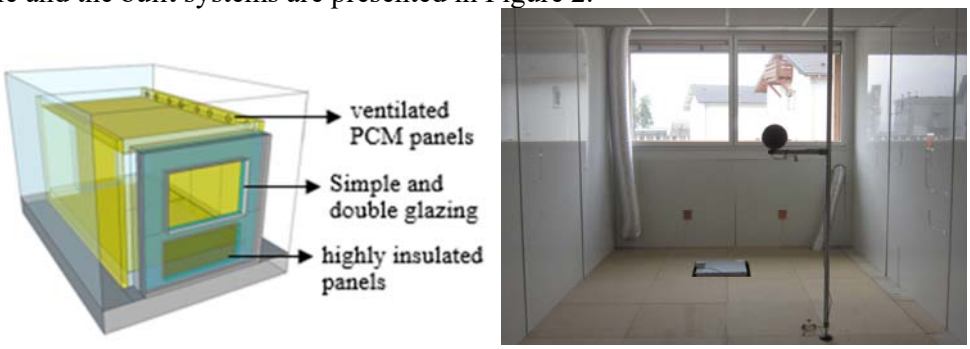

Figure 2: Illustration of the test cell at CEA INES with the photo of the built system.

Before the system was set, the test cell at INES included a simple glazed window on the south (non insulated) wall. The PCM wallboards are fixed against the East and West walls of the test cell. Each PCM panel has two openings in the lower part for the air inlet and two openings in the upper part for the air outlet. The air is taken from outside, circulate inside the PCM panels and is rejected to the outside through a sealed duct network. No air exchange is allowed between wallboards and room air.

The cell is instrumented with 29 thermocouples and 6 flux meters. One PCM panel studied more precisely is equipped with 11 thermocouples and 2 flux meters. Each of the two insulating panels are instrumented with 2 flux meters. The windows have 3 thermocouples. At the centre of the cell are installed a PT100 probe and a black globe able to measure the radiative temperature. The data recording frequency is a minute.
The ventilation was first activated in May 2016 and the window blinds were activated in July. The conditions of wallboard ventilation activation are:

- Inoccupation period (20h-7h)
- $T_{int} > 24$ °C
- $T_{int} - T_{ext} > 5$ °C.

The first observation was about the PCM wallboard ventilation's efficiency. On average, the indoor temperature decreases of 3.5 °C during the night when the ventilation is activated, and of only 0.5 °C when the conditions for activating the ventilation are not met. However, this is not sufficient to maintain a comfortable temperature in the room.
Figure 3 shows a period when the system was fully efficient. The indoor temperature was 24.5 °C in the evening of June 18th. The ventilation was activated during 8 hours. The surface temperature of the PCM panels decreased until 21 °C. This is in theory sufficient for the PCM to release 65% of its latent energy (peak solidification point being 22.5°C). The recovered storage potential has the effect of limiting the increase of the indoor temperature the following day (June 19th).
During this day the total solar gains were about 50% higher than at 18/06. However, the ventilation and the activation of the phase change allow the indoor temperature to stay below 23.5°C during 19/06 and the surface temperature to increase twice as less as the day before.

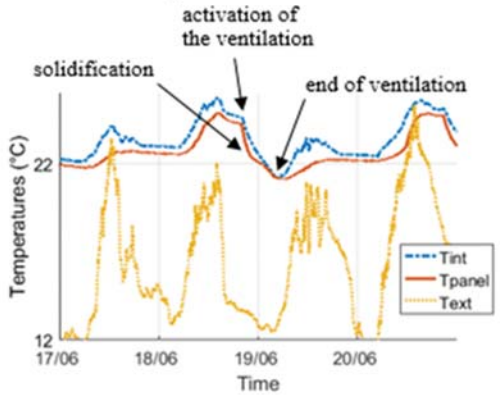

Figure 3: Combination of wallboard ventilation and phase change activation on 18th of June

Table 1: Effect of wallboard ventilation at June 18th

	18th June	**19th June**
Direct and diffuse solar radiations (Wh.m-2)	4009	5965
Mean outdoor temperature (°C)	16.8	18.3
Mean indoor temperature (°C) from 8AM to 7PM	24.6 °C	22.6 °C
Increase in the surface temperature of the panels from 8AM to 7PM	2.0 °C	0.9°C

The effect of the system on thermal comfort also lies in the fact that the surface temperature remains stable when the PCMs are melting. Thanks to the natural convection in the room, the wallboards absorb a significant amount of heat from the indoor air. However the closer the PCM is to its melting peak temperature during the warming period of the day, the higher the gap between the indoor air temperature and the surface temperature is. This enhances the "cold wall sensation" which is beneficial for the summer thermal comfort. On Figure 4 the difference between the indoor temperature and the wallboards' temperature (on average from 8AM to

7PM) is plotted as a function of the average wallboards' temperature (on average from 8AM to 7PM).

$$\left(T_{int} + T_{pan}\right)_{av} = \frac{1}{11\text{h}} \int_{8\text{h}}^{19\text{h}} \left(T_{int} - T_{pan}\right) (\text{t})\ \text{dt} \quad (1)$$

$$T_{pan_{av}} = \frac{1}{11\text{h}} \int_{8\text{h}}^{19\text{h}} \text{Tpan(t)}\ \text{dt} \quad (2)$$

Each point represents an occupation period of a day from February to July 2016. Only the "warming" days - defined as when the indoor temperature is 1°C higher at 7PM than at 8AM - are plotted.

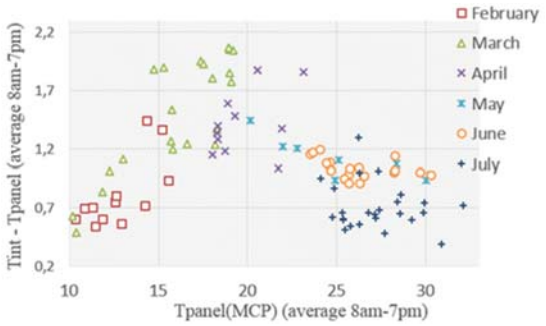

Figure 4: Difference between the indoor temperature and the panels' temperature – average from 8am to 7pm – function of average panel temperature for the days from February to July 2016

In June, the average gap between the indoor temperature and the mean wallboard temperature during the "warming days" varies between 0.6°C and 1.2°C. In March, it exceeds three times more, over 2 °C.

This has a positive effect on thermal comfort since when the latent heat storage is active, the perceived temperature (which depends on the surface temperature) is lower than the air temperature. This perceived temperature is close to the operative temperature defined as follows:

$$T_{op} = T_{int}\alpha + T_r(1 - \alpha) \quad (3)$$

with

- $\alpha = \frac{h_c}{h_c + h_r}$ a coefficient between 0 and 1 depending on the convective (h_c) and radiative (h_r) heat exchanges in the room.
- T_{int} the indoor temperature
- T_r the radiative temperature measured with a black globe probe

In a room where the air speed does not exceed 0.2 m.s^{-1}, α is approximately 0.5. That is why the perceived temperature is often considered as the average between the air temperature and the radiative temperature (close to the surface temperature). Although the air temperature increases, the perceived temperature remains more stable and comfortable. But this positive effect is observed during the periods when the need for cooling are not significant.

The goal of the following part is to evaluate the evolution of the thermal equivalent capacity of the PCM wallboards during the year. The theoretical thermal capacity $C_p(T)$ of the PCM is deduced from the data given by the PCM supplier. For every minute of the day, a mean panel temperature is calculated (from thermocouples installed in the test cell on both sides of two different panels). This wallboard temperature can be associated with an equivalent thermal capacity using the theoretical function $C_p(T)$. The assumption is made that the PCM's temperature is similar to the temperature of the panels' surface. More specific measures show that the difference between the surface temperature and the PCM temperature is limited (lower than 0,5 °C), due to the high conductivity of the panel. The goal is to determine the evolution of the thermal capacity over the year period, more specifically over the summer.

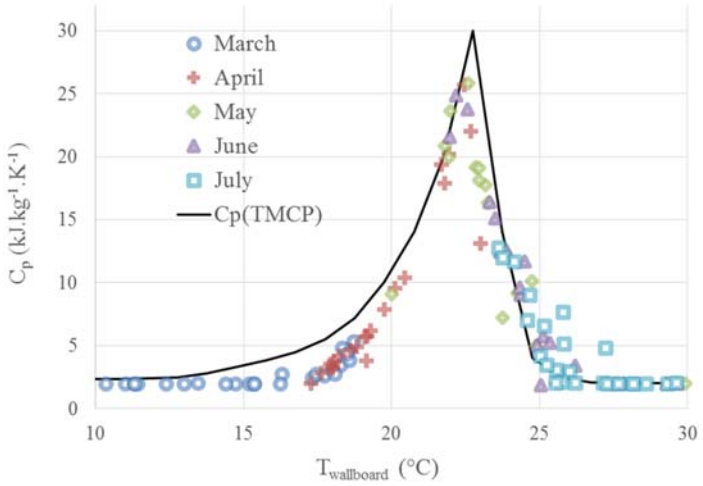

Figure 5: Average equivalent thermal capacities of the PCM panel during the days from Mars to July 2016

The higher the average thermal capacity of the panel is, the more the latent heat (or storage potential) is exploited during a day. The measures of the panels' temperature show that the thermal capacity is highest during the warmest days of April, or the coolest days of May and June. The three highest points for the month of June (triangles) corresponds to the period plotted in Figure 5. Since the priority of the system is to limit the thermal discomfort, it is not satisfying to note that during the warmest days of May and June or during the whole month of July, the activation of the phase change is very limited. During the warmest periods of the year, when the need for cooling is most important, the PCM remain melted. Figure 6 shows the frequencies of the physical states from March to July of 2016. These states are defined using the thermal equivalent capacity of the PCM and assuming that the average surface temperature of the panels is identical to the PCM temperature (Table 2).

Table 2: PCM phase dependence on temperature

Solid	**Phase change**	**Liquid**
T<19.1°C	19.1°C < T < 24.25 °C	T>24.25 °C

The ventilation of the PCM panels was active after the 11 May and the blinds were activated in early July. This chart confirms that the latent heat storage is exploited mainly in April and May. The activation of phase change is frequent when the need for cooling is not the most important. During the warmest periods of the summer, the ventilation is not sufficient to solidify the PCM. Thus, the night ventilation of wallboards fulfils its first aim to decrease the indoor temperature during the night, but not its second one which is to reactivate the inertia potential of the PCM panels. The combination of ventilation and phase change activation is not frequent enough during the summer. This was improved by combining the presented prototype by night ventilation of the room. It requires to use two independent ventilation systems: one for wallboards' ventilation and one for room free cooling. These results are not involved in this paper. To complete the study of wallboards set up as standalone problem, simulations were performed to observe the influence of the melting temperature of the PCM on the thermal comfort.

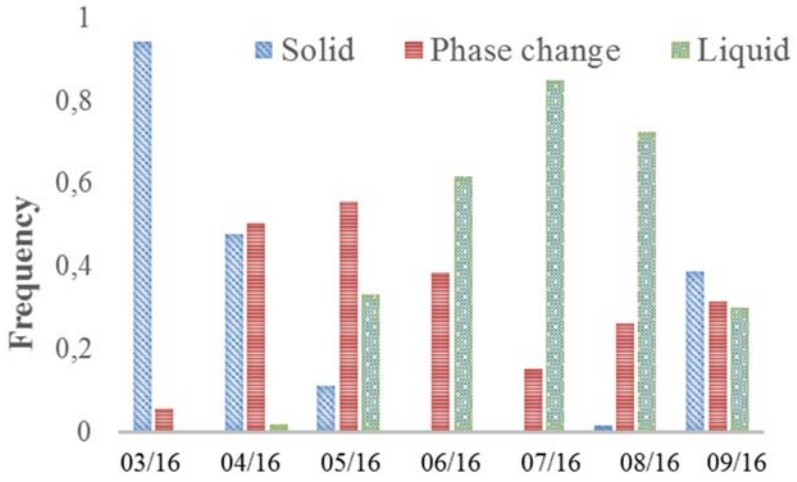

Figure 6: Monthly frequencies of each of the PCM physical states from March to July 2016

3 MODELISATION OF THE PCM PANEL

The aim of this part was to create a numerical model of the honeycomb wallboard that can be used in dynamic thermal simulation. The goal was to determine the vertical profile of the convection coefficient in the air cavity in the panel (along the direction called x) during ventilation to quantify the convection heat transfer between the ventilated air and the sides of the cavity.

Each real panel is separated in two half panels to allow two air flows to circulate from the bottom to the top. A ventilated cavity (dimensions 0.51m x 2.5m x 0.03m) which corresponds to a half panel is considered. This cavity is divided in ten parts vertically. Each tenth of panel is a zone characterized by its flow rate (identical for each part), its air inlet temperature and its air outlet temperature. An air flow rate is chosen as input to the model. The Reynolds number is calculated based on the determination of a hydraulic equivalent diameter deduced from the geometry of the wallboard, presented by equation (4).

$$Re = \frac{V.Dh}{\nu} \tag{4}$$

The Reynolds number is used to determine the flow regime, in this case laminar or transitional:

- Laminar if Re < 2500
- Transitional if 2500 < Re < 10000

From here we determine the vertical profile of the Nusselt number Nu(x). The configuration associated is that of a forced convection through a rectangular duct. In case of transitional regime, h(x) is calculated separately assuming a fully laminar and a fully turbulent regime. Then, the h(x) associated with a transitional regime is calculated by linear interpolation depending on position of the Reynolds number in the interval [2500, 10000] (Incropera et al., 2013). For a laminar regime, experimental determinations of the Nusselt number are presented by Wilbulswas (Wilbulswas, 1966). The results correspond to a configuration of a forced convection in a rectangular cavity. The Nusselt number is given as a function of:

- $\zeta = \frac{\mathbf{b}}{\mathbf{a}}$ where a = 0.51m and b = 0.03m are the dimensions of the section of the ventilated cavity perpendicular to the flow
- $x^* = \frac{x}{Dh\ Re\ Pr}$ where x is the vertical position in the panel, Dh the hydraulic diameter of the cavity, Re the Reynolds number and Pr the Prandtl number characterising the flow.

For the turbulent regime, the Dittus and Boelter correlation is used (equation (5)):

$$Nu(x) = 0.023\ Re^{0.8} Pr^{0.4} \tag{5}$$

To take into consideration the development of the flow in the entry region (x/Dh < 60), the correlation can be approximated as:

$$Nu(x) = 0.023\ Re^{0.8} Pr^{0.4}\ (1+(\frac{Dh}{x})^{0,7}) \quad (6)$$

Finally, for each rate flow expressed in air changes per hour (ACH), the profile of the Nusselt number leads to the profile of the convection coefficient h(x):

$$h(x) = \frac{Nu(x).\lambda}{Dh} \quad (7)$$

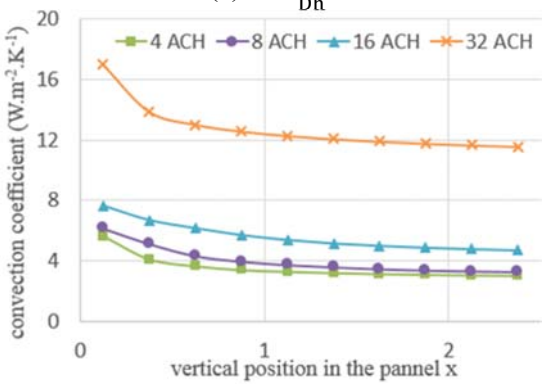

Figure 7: *Vertical profile of the convection coefficient for the thermal transfer between the air and the sides of the panel cavity*

4 SIMULATION OF THE TEST ROOM

4.1 Model of the room (EnergyPlus)

A model of the test cell at INES has been created with EnergyPlus. The Table 3 details the main parameters entered in the model. The East and West walls containing the PCM panels are also dived in ten thermal zones as described above, in order to model the air flow induced by the night ventilation with a satisfying precision. The vertical profile of the convection coefficient in the ventilated cavity is entered in the model of the test room.

Table 3: Parameters of the test cell for simulation

PARAMETER	VALUE
Test cell	
V cell volume	31.7 m3
Insulated exterior walls	
U thermal transmittance	0.0875 W.m-2.K-1
S surface	53.4 m-2
PCM panels	
λ conductivity	2.50 W.m-2.K-1
ρ density	250 kg.m-3
Concrete block wall (South)	
U thermal transmittance	5.50 W.m-2.K-1
S surface (incl. window)	7.77 m2
Additional layer including insulating panels	
U thermal transmittance	0.0171 W.m-2.K-1
S surface (incl. window)	7.77 m2
Combination of existing and added glazed windows (South)	
U thermal transmittance	1.15 W.m-2.K-1
g solar factor	0.225
Infiltration	
I infiltration rate	0.08 ACH

The data sheet of the PCM (Micronal® DS 5400) indicates experimental measures of the equivalent thermal capacity of the PCM. The enthalpy is determined by integrating the thermal capacity and entered in EnergyPlus in discretised form, as shown in Figure 8. The hysteresis observed by the difference between the peak melting temperature and solidification (supercooling) cannot be entered in the software because one material can be associated with one enthalpy curve only, but this phenomenon remains limited for paraffin.

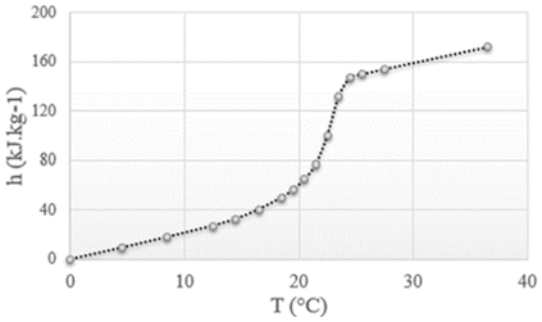

Figure 8: PCM enthalpy function of the temperature

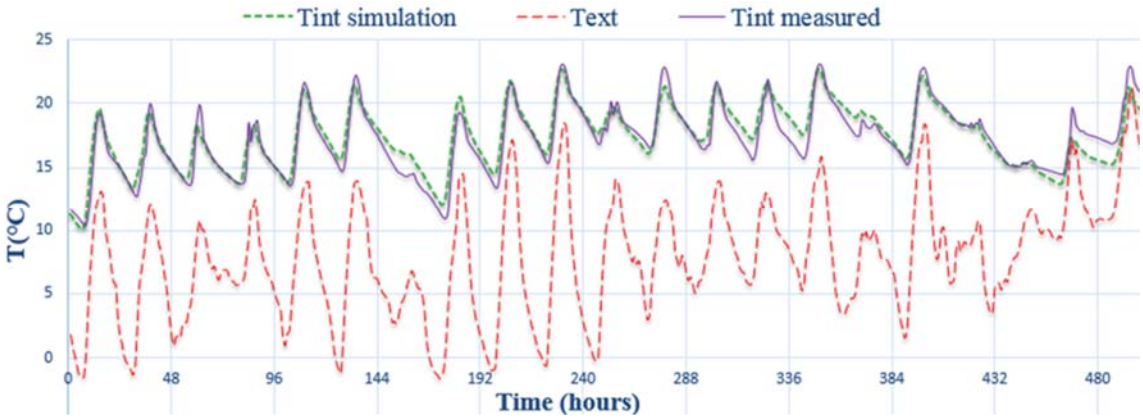

Figure 9: *From measurements: inside and outside temperatures; from simulation: inside temperature; between April 15th and April 30th of 2016 without night ventilation*

To save simulation time, a simplified model was also created, containing only two thermal zones, representing PCM wallboards on the East and West walls. In this model, the average value of the vertical profile h(x) are entered in EnergyPlus.

4.2 Validation of the model: measurements and simulation comparison

The model of the test cell is integrated in an EnergyPlus simulation using the weather file created from the data measured by the weather station at INES. These data include dry bulb temperature, dew point temperature, relative humidity, atmospheric pressure, wind speed and direction, rain, direct and diffuse solar radiation. The results of the simulations are confronted with the recorded measures from the real test cell. The mean average error between the indoor temperatures simulated and measured calculated over 1561 hours arbitrarily chosen between February and April 2016 is:

$$\frac{1}{T}\int_T |\text{Tint, sim.} - \text{Tint, meas.}|\, dt = 0.81\ °C \quad (8)$$

Figure 9 compares the indoor temperature of the test cell obtained by simulation and by measurements between the 10th and the 30th of April, 2016.

4.3 Impacts of different parameters on the thermal comfort

The indicator used in this part is called integrated thermal discomfort level and is defined by:

$$ITDL_{Tlim} = \frac{1}{T}\int_T e(t)\, dt \quad (9)$$

With:

- Tlim a limit indoor temperature of comfort (chosen here between 25 and 28 °C)
- e(t) = (Tint – Tlim) when Tint > Tlim and e(t) = 0 otherwise, with Tint(t) the indoor temperature
- T the occupation periods (8h-19h) cumulated from June to August

This indicator takes into consideration both the cumulated periods of thermal discomfort and the degree of discomfort considering to what extent the interior temperature is higher than the limit of comfort. It can be expressed in °C hours or °C days.
For the following simulations, the model of the test cell described above is used. For each series of simulation, one parameter only is modified. At first, the phase change temperature of the PCM is the only varying parameter. The total value of the latent heat is unchanged and the thermal capacity is changed as:

$$Cp_{27}(T) = Cp_{25}(T-2) = Cp_{23}(T-4) \quad (10)$$

The airflow rate is fixed to 8 ACH and the ventilation is active from 22pm to 5am every night. The results presented in Figure 10 show that the choice of the phase change temperature has a significant impact on the efficiency of the system. The configuration of the test cell (south orientation, adiabatic walls) and the climate of Rhône-Alpes region is more adapted to a PCM changing phase at 27 °C than at 23 °C if we do not combine the wallboard insulation with room night ventilation. The simulation shows that the thermal discomfort above 26 °C is reduced by nearly 65% with a PCM changing phase at 27 °C rather than at 23°C.

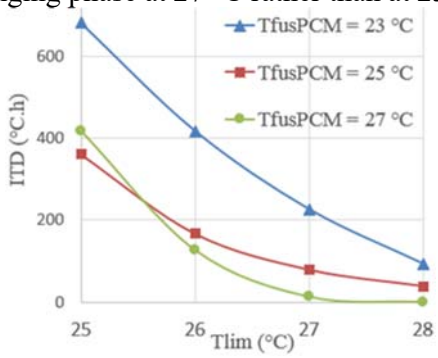

Figure 10: Integrated thermal discomfort levels for different phase change temperatures

On Figure 11 is plotted the results of the simulation for a melting temperature of 23°C (red) and 27°C (green) from the 1st to the 11th of July 2016. During the five first day when the average outside temperature is 20°C, the thermal mass is more important for the phase change temperature of 23°C. The variations of the inside temperature are much reduced compared to the configuration with the PCM changing phase at 27°C. Yet there is no effect on the thermal discomfort above 26°C because in both configurations the indoor temperature remains below this limit (represented in black). The thermal discomfort above 26°C that corresponds to the area between the 26°C limit and the curve of the indoor temperature is notably higher for a change phase temperature of 23°C than 27°C. In order to reduce the thermal discomfort in July in the configuration of the test cell and for the climate of Lyon (France), a melting temperature of 27°C is more adequate than 23°C without room night ventilation.

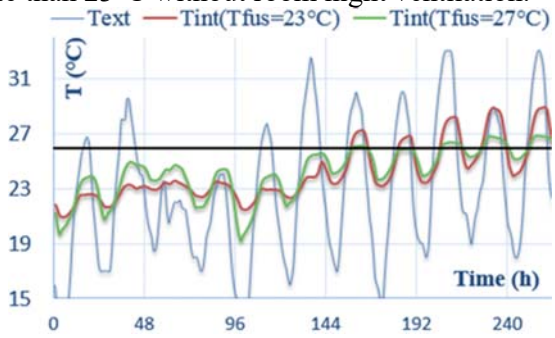

Figure 11: Outside temperature and Inside temperatures with phase change temperatures of 23°C and 27°C, from a simulation of the test cell using a weather file of Lyon (Rhône-Alpes, France) from 2015

In a second test, the intensity of the air flow rate (and the convection coefficient associated in the model) is the only varying parameter. The PCM temperature is set to 27 °C. Figure 12 shows that this parameter has a major impact on the thermal discomfort and thus on the efficiency of the system. For example, intensifying the ventilation flow rate from 2 to 4 ACH allows a decrease by half of the integrated thermal discomfort level above 26 °C.

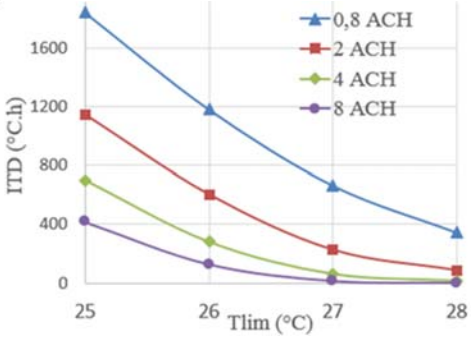

Figure 12: Integrated thermal discomfort levels for different airflow rates

5 CONCLUSIONS

Results of the paper show that the box in the box concept is able to replace air-conditioning by free cooling in the studied temperate climate. Nevertheless, wise combination with space ventilation is crucial to obtain competitive results for hot periods. Numerical simulations show that a PCM changing phase at 27 °C can decrease the "integrated thermal discomfort level over 26°C" (ITDL26) by 65% compared to a PCM changing phase at 23°C. Numerical analysis also emphasizes that rise the ventilation rate of the developed panels from 4 ACH to 8 ACH reduce the ITDL26 by 50%. Results of combination of the presented solution with room night ventilation are object of an upcoming analysis and are intentionally not included in this paper by lack of space for detailed description.

6 ACKNOWLEDGEMENTS

The authors express their gratitude to BPI for its financial support of this study under the grant of FUI AAP14-F1401002B.

7 REFERENCES

Evola, G., Papa, N., Sicurella, F., Wurts, E. (2011). *Simulation of the behaviour of phase change materials for the improvement of thermal comfort in lightweight buildings*, Proceedings of Building Simulation 2011, Sydney, Australia.

Evola, G., Marletta, L., Sicurella, F. (2014). *Simulation of a ventilated cavity to enhance the effectiveness of PCM wallboards for summer thermal comfort in buildings*, Energy and Buildings 70,

Hasse, C., Grenet, M., Bontemps, A., Dendievel, R., Sallée, H. (2011). *Realization test and modelling of honeycomb wallboards containing a Phase Change Material*, Energy and Buildings 43, 232-238.

Zhang, Y., Zhou, G., Lin, K., Zhang, Q., Di, H., 2006. *Application of latent heat energy storage in buildings: State-of-the-art and outlook*, Building and Environment 42,

Wilbulswas, P. (1966), Laminar flow heat transfer in non circular ducts, Ph.D. thesis, London University, London

Incropera, P., Dewitt, D., Bergman, T., Lavine, (2012). *Principles of heat and mass transfer*, Seventh Edition, p.545-546